

Tadeusz RODZIEWICZ^{1*}, Josuke NAKATA², Kenichi TAIRA², Aleksander ZAREMBA³
and Maria WACŁAWEK¹

IMPACT OF THE SOLAR IRRADIATION ANGLE ON THE WORK OF MODULES WITH SPHERICAL CELLS - SIMULATION

WPLYW KĄTA PADANIA PROMIENI SŁONECZNYCH NA PRACĘ MODUŁÓW Z OGNIWAMI SFERYCZNYMI - SYMULACJA

Abstract: The main purpose of all PV modules is to convert solar energy into electricity, but in the era of building integrated photovoltaics, there are additional opportunities to use them. The use of them as a composite of architectural structures in the form of facade cladding, roofing, stained glass windows or noise barriers on highways, in addition to generating electricity embellish also the aesthetic value of the facilities. However, these atypical their use, cause that the modules should have quite different properties then in the traditional application, which is related to their unusual way of positioning. Particularly for structures such as the modules made of spherical cells with the two active planes of operation. The article presents a comparison of the results of simulation of module with two active surfaces containing spherical solar cells in an open space in relation to a typical flat photovoltaic module. A comparison of its work with different orientation and inclination. Article shows the basic difference in its properties occurring at some settings in relation to a typical module and makes predictions about its future use.

Keywords: PV cells, PV modules, 3D, modelling, monitoring

Introduction

Kyosemi Corporation (Japan) has patented a new design of photovoltaic cells called SPHELAR[®]. Individual cells are formed as the silicon spheres (hence the name of cells: spherical or 3D) having a diameter of approx. 1 mm, able to absorb solar radiation incident at different angles. The use of 3D design resulted in very good use of diffuse component of solar radiation.

In Figure 1a is shown in cross-section SPHELAR[®] cells [1-3]. It is composed of p-type monocrystalline silicon, wherein using doping of element from group V is prepared a thin coat of n+ type. At the border area of the shell and kernel appears p-n junction, in

¹ Division of Physicochemical Research, Faculty of Natural Sciences and Technology, University of Opole, ul. kard. B. Kominka 6, 45-032 Opole, Poland, phone +48 77 401 60 42, fax +48 77 401 60 51, email: maria.waclawek@o2.pl, trodziewicz@wp.pl

² Kyosemi Corporation, 385-31 Toiso, Eniwa, Hokkaido 061-1405, Japan, email: taira@kyosemi.co.jp

³ Chair of Industrial Electrical Engineering, Faculty of Electrical Engineering, Czestochowa University of Technology, al. Armii Krajowej 17, 42-200 Czestochowa, Poland, email: zaremba@el.pcz.czest.pl

*Corresponding author: trodziewicz@wp.pl

which there is an electric field necessary for the separation of generated electric charge carriers. After etching the lower and upper part of the cell is sprayed small electrode: silver and aluminium, thereby forming the electrical contact connection of the emitter (top) and the base (core) of the cell. The thus formed electrical contacts allow the combination of cells in series and/or parallel to form a SPHELAR[®] module. Depending on the design, the modules have different characteristics. The most common is formed in the shape of a dome as shown in Figure 1b-c or, as a flat module with two active surfaces.

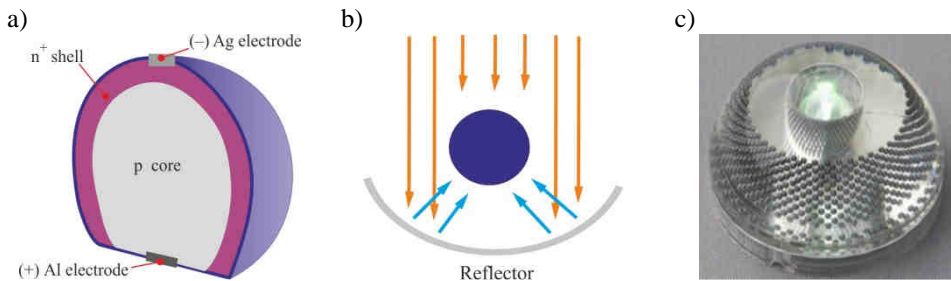


Fig. 1. SPHELAR[®] cell [1-3]: a) cross-section; b) the idea of using hemispherical casing as a reflector for 3D cell; c) photo of dome-shaped SPHELAR[®] module

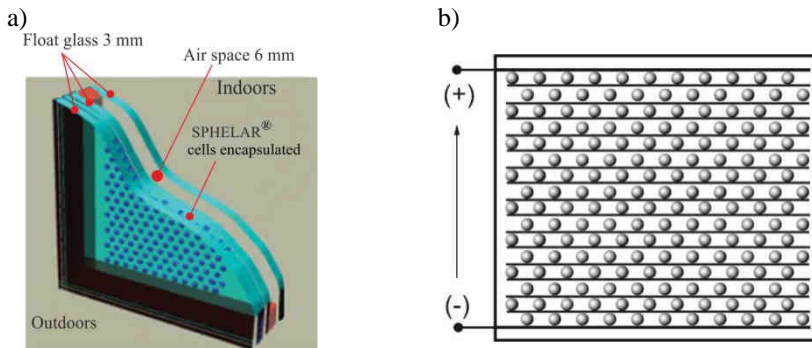


Fig. 2. Window with capsuled SPHELAR[®] cells (figures do not preserve proportion): a) construction; b) a matrix of wiring in SPHELAR[®] cell [3]

In the case of modules having a flat structure, due to the ability to do different patterns from the cells 3D and obtained different coefficients of transparency, it appears that this type of design is ideal for use as a facade cladding of buildings, stained glass or roof windows and noise barriers used on motorways and highways.

Figure 2a [3] provides an example of composite window with built-in module made of SPHELAR[®] cells. Between the two glass plates 3 mm thick, with a low iron content, is placed matrix of 3D cells separated by a thin layer of plastic and hermetic foil EVA (copolymer of ethylene with vinyl acetate). The cells are electrically connected as shown in Figure 2b. 6 mm layer of air between the inner and outer glass provides a window unit for the required coefficient of thermal conductivity. Transparent window depends on the pattern arrangement used and the number of cells hermetically sealed in a SPHELAR[®]

module [3]. The more cells, the more electricity generates window module, however, has lower transparency.

Research methodology

The study of the effect of the use of two active surfaces in a 3D spherical module for different angles of its inclinations (facing) on its parameters was made with reference to a typical flat PV module. The research was performed as a simulation study to estimate the potential properties of the module under test, resulting from the assumed design and to determine its optimal future use.

Study of the effect of the application of the two active surface in the module with spherical cells for different angles of inclination (focus) on the parameters obtained by him were made in comparison to a typical flat PV module. Tests were performed as a simulation study to estimate the potential properties of a module resulting from the adopted design and to determine its optimal future use.

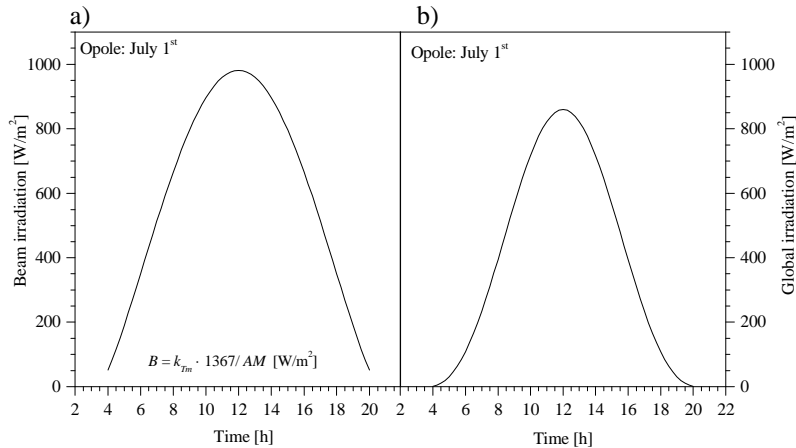


Fig. 3. a) Distribution of the direct component as a function of time (the surface perpendicular to the beam) and b) the value of the global solar irradiation on a horizon surface (July 1st, Opolo)

The simulations were performed for the following conditions: time - July the 1st, area - Opolo (latitude 52°N, longitude 17°E), type of day - very sunny day. In studies, the following simplifications were made: both modules do not take into account the radiation reflected from the terrain elements, diffuse component ($G_S(t)$) is 10% of the direct component, there are stable: spectral distribution during the day and an index of purity sky (k_{Tm}).

The characteristics of the distribution of solar radiation in the upper atmosphere (G_d), distribution of direct ($B(t)$) and global (G_0) component on the surface of the Earth (Fig. 3) are dependent on the instantaneous values of coefficients: the air mass (AM) and transparency atmosphere (k_{Tm}) in the following way [3-7]:

$$G_d = I_0 (1.00011 + 0.034221 \cos \alpha_d + 0.00128 \sin \alpha_d + 0.000719 \cos 2\alpha_d + 0.000077 \sin 2\alpha_d) \quad (1)$$

I_0 - solar constant $1367 \pm 7 \text{ W/m}^2$ (World Meteorological Organization, Commission of Measurements and Method of Observation, 8 session, Mexico City, 1981 [8]);

$$B(t) \equiv k_{rm} G_d / AM \quad (2)$$

$$G_0(t) = B(t) \cdot [\cos(\varphi) \cos(\delta) \cos(\omega) + \sin(\varphi) \sin(\delta)] \quad (3)$$

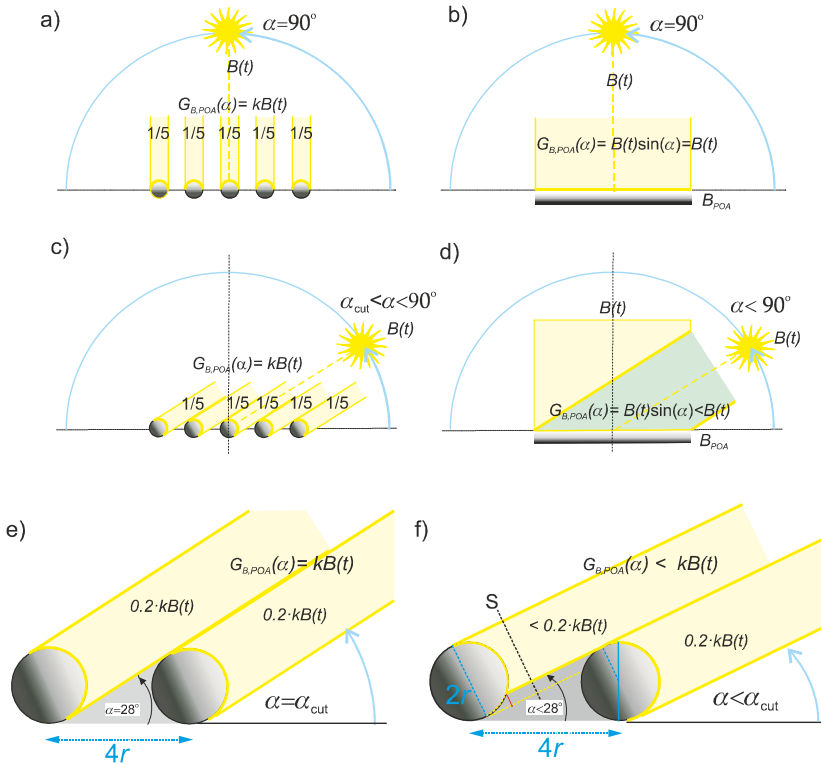


Fig. 4. Modelling of changes in the effective flow direct component as a function of Sun elevation angle for: a) modules with SPHELAR[®] cells with two active surfaces of work (k - factor of packing cells defined as the ratio of area of cells in a module to the total area module); b) typical photovoltaic module with one active surface work; the impact of changing the Sun elevation angle (α) into the stream of solar radiation falling on the spherical (c) and plane module (d). The phenomenon of mutual shading of spherical cells for the Sun elevation angle: e) equal to the limit of the working angle $\alpha = \alpha_{cut}$ and f) lesser than the limit of the working angle $\alpha < \alpha_{cut}$. The first rows of cells are shaded by the frame and sealing of the module

The value of the intensity of the radiation on the inclined plane of the modules is the sum of direct and diffuse component, i.e.:

$$G_{0,POA}(t) = G_{B,POA}(t) + G_{S,POA}(t) \quad (4)$$

where useful values of streams for components of the solar radiation on a surface of the module, are determined using the following models of physical phenomena:

A. **Model of the impact of the direct component of solar radiation** on module with spherical cells and on typical flat with one active absorption surface. The value of flux of the direct component of solar radiation $G_{B,POA}(t)$ on a surface of the module is directly related to the cross-sectional area of the useful beam in plane of the module. In case of:

- 1) **standard flat modules**, the size of the stream is a function of sine of Sun elevation angle according to:

$$G_{B,POA}(t) = B(t) \sin \alpha \quad (5)$$

At noon, when the Sun elevation angle $\alpha = 90^\circ$, the value of flux illuminating the surface is equal to the flux of direct component of the radiation (see Fig. 4b, d).

- 2) **modules with spherical cells**, due to the characteristics of the sphere, the flux on the cell is constant for angles above the limit angle of work modules 3D (i.e. α_{cut}) and depends only on k - factor of packing cells (Fig. 4a, c).

In the case of modules work in conditions Sun elevation angle smaller than the limit angle of operation (Fig. 4e, f) must also be taken into account: a) the *coefficient of mutual shading spherical cells* associated with a their *radius of shading* (Fig. 5), and b) the effect of shading the first row of cells by the structural elements of the module (i.e. the frame). Later in this article, was adopted the simplification assuming the same character of shading for the first row of cells, what other.

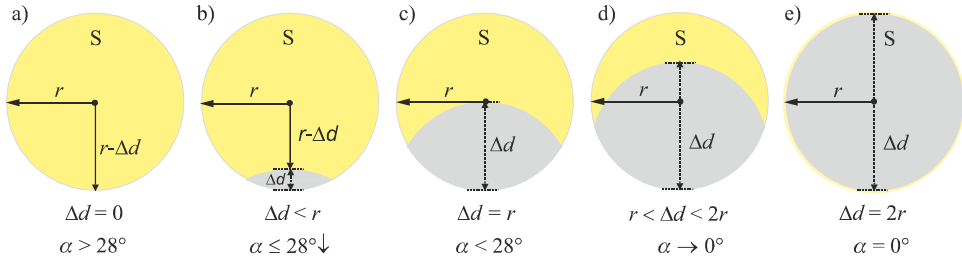


Fig. 5. The impact of mutual shading of cells on the section of useful direct component for different values of shading: a) the lack of shading, i.e. for Sun elevation angle $\alpha > 28^\circ$ (i.e. when the value of the shading radius $\Delta d = 0$), b) for small shading, i.e. when the Sun elevation angle is around the limit $\alpha \leq 28^\circ$ (i.e. for $\Delta d \ll r$), c) the average shading, i.e. for $\alpha < 28^\circ$ and when $\Delta d = r$, d) big shading, i.e. the angle is going to zero ($\alpha \rightarrow 0^\circ$), and when the shading radius $\Delta d \in (r, 2r)$; e) a full shading, i.e. the angle of elevation of the Sun is zero ($\alpha = 0^\circ$) and the $\Delta d = 2r$

Transfer function of direct component due to mutual shading of cells in the 3D module can be presented in the form:

$$K(\alpha) = \frac{S(\alpha > \alpha_{cut})}{S(\alpha)} = \begin{cases} 1, & 90^\circ \geq \alpha > \alpha_{cut} \\ \frac{S(\alpha)}{\pi r^2}, & 0 \leq \alpha \leq \alpha_{cut} \end{cases} \quad (6)$$

Then, the value of the useful stream of direct component in this module takes the form of dependence (7):

$$G_{B,POA}(\alpha) = \begin{cases} kB(t), & \alpha > \alpha_{cut} \\ kK(\alpha)B(t), & \alpha \leq \alpha_{cut} \end{cases} = \begin{cases} kB(t), & 90^\circ \geq \alpha > \alpha_{cut} \\ k \frac{S(\alpha)}{\pi r^2} B(t), & 0 \leq \alpha \leq \alpha_{cut} \end{cases} \quad (7)$$

For such adopted model, specific dependencies for the transmittance and the elevation angle of the Sun were presented, i.e.:

- The value of limit work angle α_{cut} for spherical module (Fig. 6a)

To simulation was assumed value of the spacing between cells equal to the diameter of the cells $2r$, which is a similar to value in real SPHELAR[®] module.

For such assumptions, in Figure 6a were shown an algorithm of determination of the value of the minimum elevation angle of the Sun, where still there is no mutual shading to cells, and the value obtained for the construction of the limit working angle (8):

$$\begin{aligned} \operatorname{tg}\left(\frac{\alpha_{cut}}{2}\right) &= \frac{r}{4r} = 0.25 \rightarrow \frac{\alpha_{cut}}{2} = \operatorname{arc\,tg}(0.25) \\ \alpha_{cut} &= 2 \operatorname{arc\,tg}(0.25) \approx 28^\circ = 0.4884 \operatorname{rad} \end{aligned} \quad (8)$$

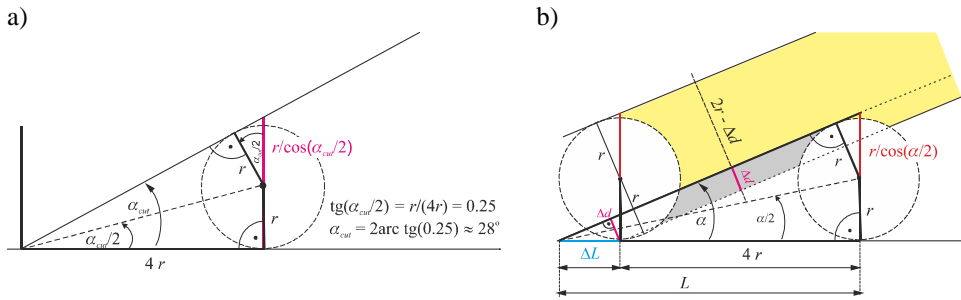


Fig. 6. Determination of: a) limit working angle (α_{cut}) for SPHELAR[®] modules; b) the shading radius (Δd) as a function of Sun elevation angle (α)

- values of the shading radius for spherical cells in SPHELAR[®] module (Fig. 6b):

In the case of the Sun rising angle α lower than the limit work angle of the module (α_{cut}), the algorithm for determining the shading radius is shown on Figure 6b, i.e.:

$$\begin{aligned} \operatorname{tg}(\alpha/2) &= \frac{r}{L} = \frac{r}{4r + \Delta d}, \quad \sin(\alpha) \frac{\Delta d}{\Delta L} \rightarrow \Delta L = \frac{\Delta d}{\sin(\alpha)} \text{ or:} \\ \operatorname{tg}\left(\frac{\alpha}{2}\right) &= \frac{r}{4r + \frac{\Delta d}{\sin(\alpha)}} = \frac{r \cdot \sin(\alpha)}{4r \cdot \sin(\alpha) + \Delta d} \rightarrow \Delta d = \frac{r \cdot \sin(\alpha) - 4r \cdot \sin(\alpha) \operatorname{tg}\left(\frac{\alpha}{2}\right)}{\operatorname{tg}\left(\frac{\alpha}{2}\right)} \end{aligned}$$

or

$$\Delta d(\alpha) = \begin{cases} 0, & \text{for } 90^\circ \geq \alpha \geq \alpha_{cut} \\ r \left(\operatorname{ctg}\left(\frac{\alpha}{2}\right) - 4 \right) \cdot \sin(\alpha), & \text{for } 0^\circ < \alpha \leq \alpha_{cut} \end{cases} \quad (9)$$

In the general case, when the module is operating in a position other than the horizontal one and the phenomenon of rear illumination thereof, it is much more convenient to operate instead of the sunrise angle (α), the angle of incidence of the radiation beam to the normal of module (θ). Considering that $\theta = (90^\circ - \alpha)$ and $\sin(90^\circ - \alpha) = \cos \alpha$, is obtained:

$$\Delta d(\theta) = \begin{cases} 0, & \text{for } |\cos(\theta)| \geq \sin(\alpha_{cut}) \\ r \left(\left| \operatorname{ctg}\left(\frac{90-\theta}{2}\right) \right| - 4 \right) \cdot |\cos \theta|, & \text{for } |\cos(\theta)| < \sin(\alpha_{cut}) \end{cases} \quad (10)$$

To illustrate the correctness of the model used, Figure 7a shows the course of the shading value (i.e., the relationship graph (9)) as a function of the Sun elevation angle. In contrast, Figure 7b illustrates the general case, i.e. if the module is operating in a position other than the horizontal position and the phenomenon of rear illumination occurs. In this case, the variable α no longer indicates the angle of sunrise over the horizon, but the angle of incidence of the solar radiation beam (i.e. direct component) to the plane of the array (module) (POA).

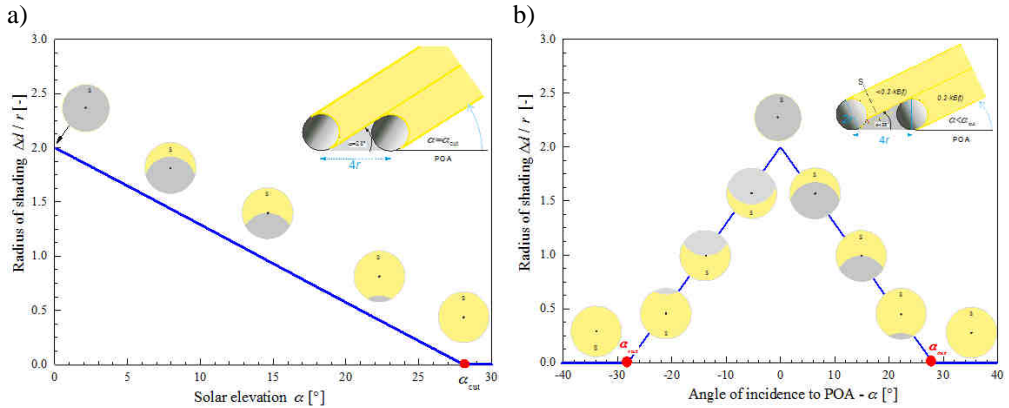


Fig. 7. The shading radius value (Δd) of the spherical cells in SPHELAR[®] module in the function of: a) the Sun's rising angle, b) the angle of incidence of solar radiation to the plane of the module (α)

- Shaded cross section area of the direct component beam (see Figure 8) and the direct radiation component transmission function for the SPHELAR[®] module:

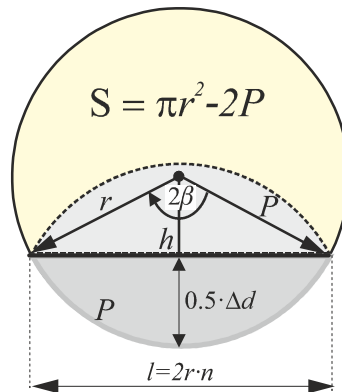


Fig. 8. Determination of effective surface of a stream beam of direct component as a function of its shading

From the detailed observation of the shape of the shade of the beam cross-section, it follows that it is an assembly of two symmetrical figures, with the axis of symmetry being a circle chord. One of them is a circle segment with a chord l . Therefore, the resulting

shaded area of the useful solar beam will be a doubled product of the area of the circle with the chord l . Using published dependencies on the fields of selected flat geometric figures (see mathematical tables), the dependence on the area of the circle segment of the chord l , is the form:

$$P = r^2(\beta - n\sqrt{1-n^2}) \quad (11)$$

where $2r \cdot n$ is the length of the chord of a circle ($n \in (0,1)$), and: $n = \frac{l}{2r}$, taking into account that:

$$\frac{h}{r} = \cos(\beta) = \frac{r-0.5\Delta d}{r}$$

is obtained:

$$\beta = \arccos \frac{r-0.5\Delta d}{r} \quad (12)$$

Also, noting that $\sin \beta = \frac{0.5 \cdot l}{r}$, $\rightarrow l = 2r \cdot \sin \beta$, then that's it:

$$n = \frac{l}{2r} = \frac{2r \cdot \sin \beta}{2r} = \sin \beta \quad (13)$$

The cross-sectional area of the useful direct component beam is in the form:

$$S = f(x) = \begin{cases} \pi r^2, & 90^\circ \geq \alpha \geq \alpha_{cut} \\ \pi r^2 - 2r^2(\beta - \sin \beta \sqrt{1 - (\sin \beta)^2}), & 0^\circ < \alpha \leq \alpha_{cut} \end{cases} \quad (14)$$

So the function of the direct component transmittance for SPHELAR[®] module, takes the form:

$$K(\alpha) = \frac{S(\alpha)}{S(\alpha \geq \alpha_{cut})} = \frac{S(\alpha)}{\pi r^2} = \begin{cases} 1, & 90^\circ \geq \alpha \geq \alpha_{cut} \\ 1 - \frac{2}{\pi}(\beta - \sin \beta \cdot \sqrt{1 - (\sin \beta)^2}), & 0^\circ < \alpha \leq \alpha_{cut} \end{cases} \quad (15)$$

And the value of the useful direct component stream described by the relation (7) takes the form:

$$G_{B,POA}(\alpha) = \begin{cases} kB(t), & 90^\circ \geq \alpha \geq \alpha_{cut} \\ kB(t) \left(1 - \frac{2}{\pi}(\beta - \sin \beta \cdot \sqrt{1 - (\sin \beta)^2})\right), & 0^\circ < \alpha \leq \alpha_{cut} \end{cases} \quad (16)$$

Or in the general case, including the backlight phenomenon of the module:

$$G_{B,POA}(\theta) = \begin{cases} kB(t), & |\cos(\theta)| \geq \sin(\alpha_{cut}) \\ kB(t) \left(1 - \frac{2}{\pi}(\beta - \sin \beta \sqrt{1 - (\sin \beta)^2})\right), & |\cos(\theta)| < \sin(\alpha_{cut}) \end{cases} \quad (17)$$

B. Model of interaction of diffused solar radiation component on spherical 3D module and typical plane module with one active surface of absorption

The value of the diffused component of solar radiation on the angled γ plane of the module is described - the dependence (18) for the typical PV module, and (19) for the module with two active planes (Fig. 9):

$$G_{S,POA}(t) = \frac{180-\gamma}{180} G_S(t) \quad (18)$$

$$G_{S,POA}(t) = G_S(t) \quad (19)$$

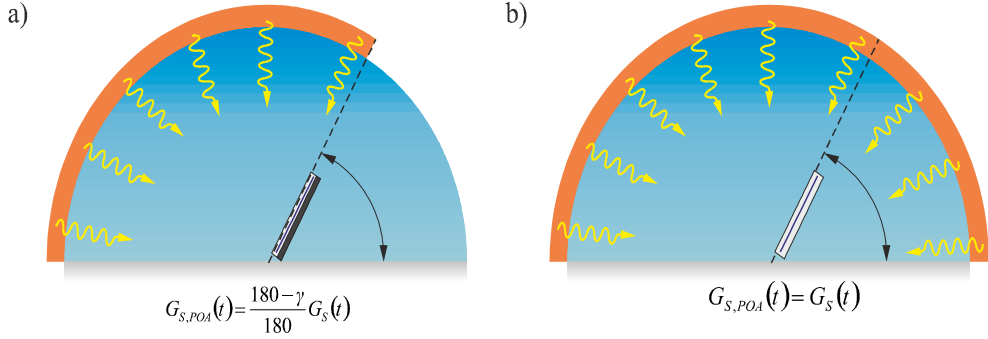


Fig. 9. The model of the distribution of diffused component (from horizon) in the surface of module as a function of inclination angle for: a) typical photovoltaic module with one active surface; b) for modules with two active work surfaces as in the flat module with SPHELAR® cells

Others necessary analytical dependencies for determining the density of the solar radiation intensity on the inclined surfaces of the modules were taken from [3-7] and is shown below:

$$t_{sol} = t_{std} + \frac{L_{st} - L}{15} + E \quad (20)$$

$$E = 3.82 \left[\begin{array}{l} 0.0000075 + 0.001868 \cos(\alpha_d) - 0.032077 \sin(\alpha_d) - 0.014615 \cos(2\alpha_d) \\ -0.04089 \sin(2\alpha_d) \end{array} \right] \quad (21)$$

$$\theta = \cos^{-1}(\cos z \cos \gamma + \sin z \cos(A_s - A_\phi) \sin \gamma) \quad (22)$$

$$z = \cos^{-1}(\cos \phi \cos \delta \cos \omega + \sin \phi \sin \delta) \quad (23)$$

$$AM = \frac{1}{\cos z + 0.0003(1.6014 - z)^{-1.356}} \quad (24)$$

$$A_s = \text{atan2} \left(\underbrace{\cos \omega \sin \phi - \cos \phi \tan \delta}_{x(t)}, \underbrace{\sin \omega}_{y(t)} \right) \quad (25)$$

$$\delta = 0.006918 - 0.399912 \cos \alpha_d + 0.070257 \sin \alpha_d - 0.006758 \cos 2\alpha_d + \\ + 0.000907 \sin 2\alpha_d - 0.002697 \cos 3\alpha_d + 0.00148 \sin 3\alpha_d \quad (26)$$

where: $\alpha_d = 2\pi(d - 1)/365$ - the angle of Earth's circulation at the orbit around the Sun [rad]; d - day number of the year, $\omega = 2\pi/24$ [rad] - the value of the Sun's position on the sky (negative in the morning, positive in the afternoon, at noon 0° and rising $15^\circ/\text{h}$); t_{sol} - sunny time (i.e. astronomical); t_{std} - local time (zonal); L_{st} - longitude appropriate for locating the time zone; L - longitude of research facility location; E - equation of time (radiations) - the correction of the duration of the astronomical period resulting from the Earth's rotation and the move on the elliptical orbit as a function of the angle of Earth's circulation around the Sun (α_d); θ - angle of incidence of sunlight on normal to the surface of the module; z - angle between solar radiation beam and normal to horizon, γ - plane of array (module) (POA), δ - the value of the declination of the Sun as a function of the angle

of the Earth's circulation around the Sun α_d ; ϕ - the geographic latitude of the location; A_φ - Azimuth of module position, A_S - azimuth of the position of the Sun on the sky.

Research results

Figure 10 shows the typical operating conditions of the modules occurring at different times of the year when they are mounted: a) on an inclined or perpendicular surface set south, and b) vertically oriented towards sunrise or sunset. A very characteristic feature is the appearance of the illumination of the back of the modules. This phenomenon is evident in the summer months in the sunrise and sunset, and the stronger the larger the slope angle of the modules (γ). In the case of modules placed in vertical position, the illumination of the rear of the module is the longest.

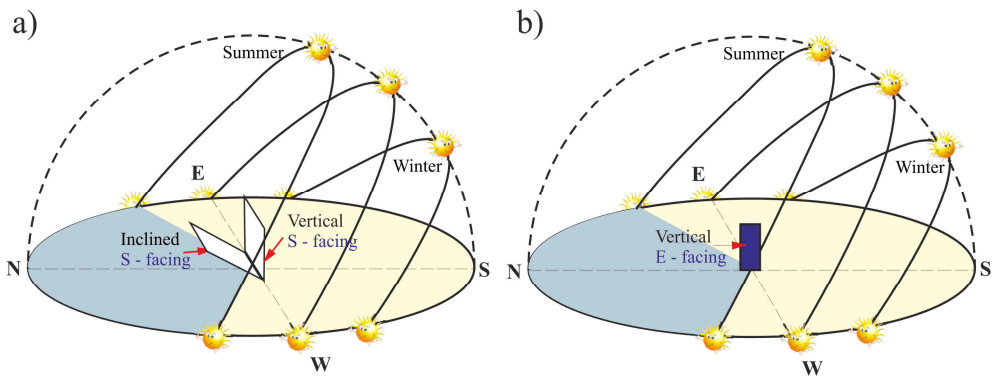


Fig. 10. Sunspot movement for particular seasons: a) southern direction of the module vertically aligned and inclined to the horizon; b) eastern orientation of the module vertically oriented

Taking into account that in the photovoltaic conversion of cells and modules, there is a linear dependence of the produced photocurrent ($I_{ph} \cong I_{SC}$) on the total solar radiation intensity ($G_{0,POA}(t)$), so the graphs of normalized value of sunlight intensity and short circuit current of illuminated cell/module are identical ($G_{0,POA}(t)_{norm} \cong I_{SCnorm}$). Therefore, later in this article these charts are treated as equivalent.

Figures 11-13 illustrate the changes of the normalized I_{SC} values during the day, depending on the angle of inclination and the orientation of the modules under study. At the same time, in Figure 11, the modules has southern, and Figures 12 and 13 have east orientation. The study was conducted for: a) SPHELAR[®] modules with two active surfaces, b) a typical photovoltaic module with one active surface.

The analysis of the results of the simulations gives the following observations:

1. SPHELAR[®] cells with two active surfaces always have better conditions for producing photocurrent than conventional modules, because:
 - In sunny days - in a wide range of changes in the angles of direct solar radiation to the normal surface of the module (i.e., for $-62^\circ \leq \theta \leq 62^\circ$) - the value of the produced photocurrent is constant (previously described phenomenon of cross sectional area of the active stream participating in the photocurrent generation - see equation (17)).

- In cloudy days, the spherical structure of the cells and having 2 active surfaces significantly improve the absorption of the diffused component from the environment (see equations (18) and (19)).

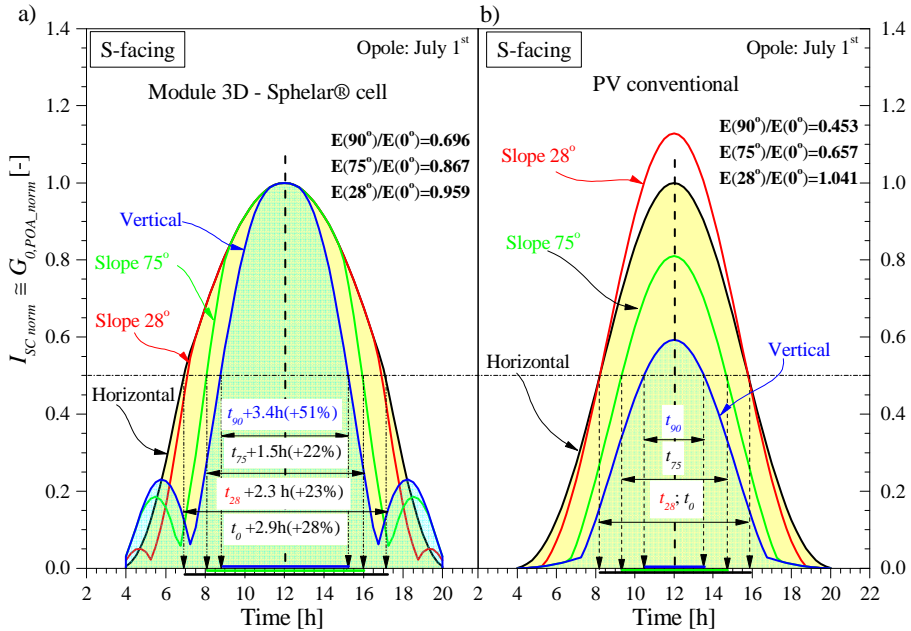


Fig. 11. Graph of the normalized I_{SC} values during the day, depending on the inclination angle of the modules. Normalisation were made to max. values of I_{SC} current from module in horizontal position, for: a) modules with SPHELAR® cells with two active surfaces, b) a typical photovoltaic module with one active surface. Modules have south orientation

2. In the early and late hours of the day, the conditions for producing a photocurrent for SPHELAR® modules with two active surfaces are significantly better than for conventional modules, as observed by the characteristic two side leaves in Figure 11a. These leaves are the result of modules working in the presence of rear solar radiation.
3. Eastern/western vertical position of modules (Fig. 12a) causes the main leaf to disappear on the I_{SC} current characteristics of the SPHELAR® modules and the growth of two side leaves. Exactly at 12⁰⁰, when the Sun is in the zenith, the normalized current is 0.1, i.e. only the diffused component of the environment is converted (see relations (4) and (19) and Figure 9b). In the case of a conventional module, it has only one side leaf (Fig. 12b), which means that it does not have good working characteristics throughout the day with this setting, i.e. it is only capable of working in one half day.

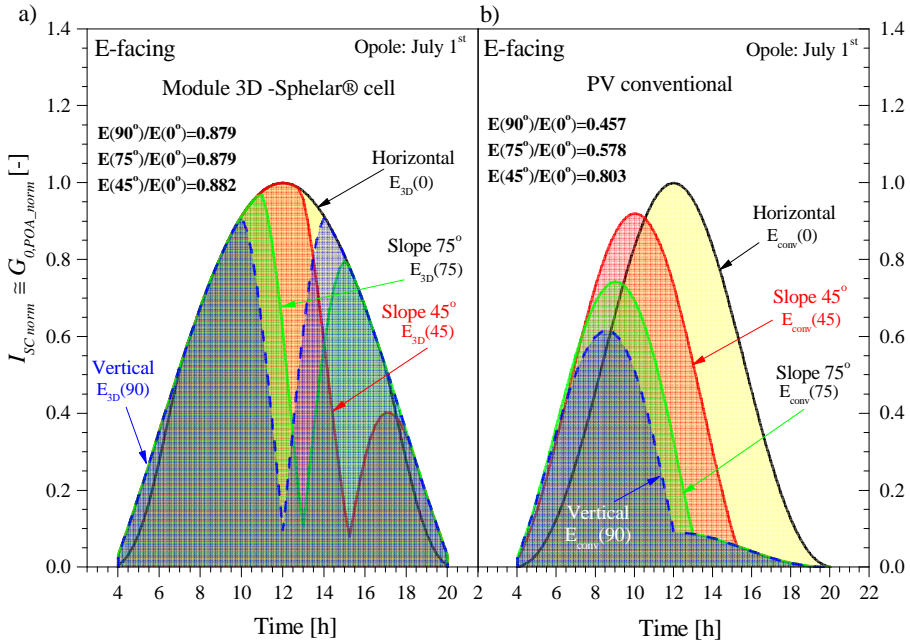


Fig. 12. Graph of the normalized I_{SC} values during the day, depending on the inclination angle of the modules. Normalisation were made to max. values of I_{SC} current from module in horizontal position, for: a) modules with SPHELAR® cells with two active surfaces, b) a typical photovoltaic module with one active surface. Modules have east orientation

4. By determining the effective work time of the module, as the time at which the value of the photocell generated is not less than half the value obtained at midday, it is stated that on a sunny summer day, SPHELAR® cells work considerably longer than conventional flat modules (Fig. 11):
 - a. In case of south position, at (Fig. 11):
 - **3.4 h**, with a vertical setting (90°), i.e. ~51% longer than conventional flat modules,
 - **1.5 h**, with an inclination 75° , i.e. ~22% longer than conventional flat modules (without consideration of side leaves),
 - **2.3 h**, with an inclination 28° , i.e. ~22% longer than conventional flat modules (without consideration of side leaves),
 - **2.9 h**, with an inclination 0° , i.e. ~22% longer than conventional flat modules.
 - b. In case of east position, at (Fig. 13):
 - **2.9 h**, with an inclination 0° (horizontal position), i.e. ~28% longer than conventional flat modules,
 - **>1.1 h**, with an inclination 45° , i.e. ~15% longer than conventional flat modules (without consideration of side leaf),
 - **4.3 h**, with an inclination 75° , i.e. ~49% longer than conventional flat modules,
 - **5.8 h**, with an inclination 90° , i.e. ~66% longer than conventional flat modules,

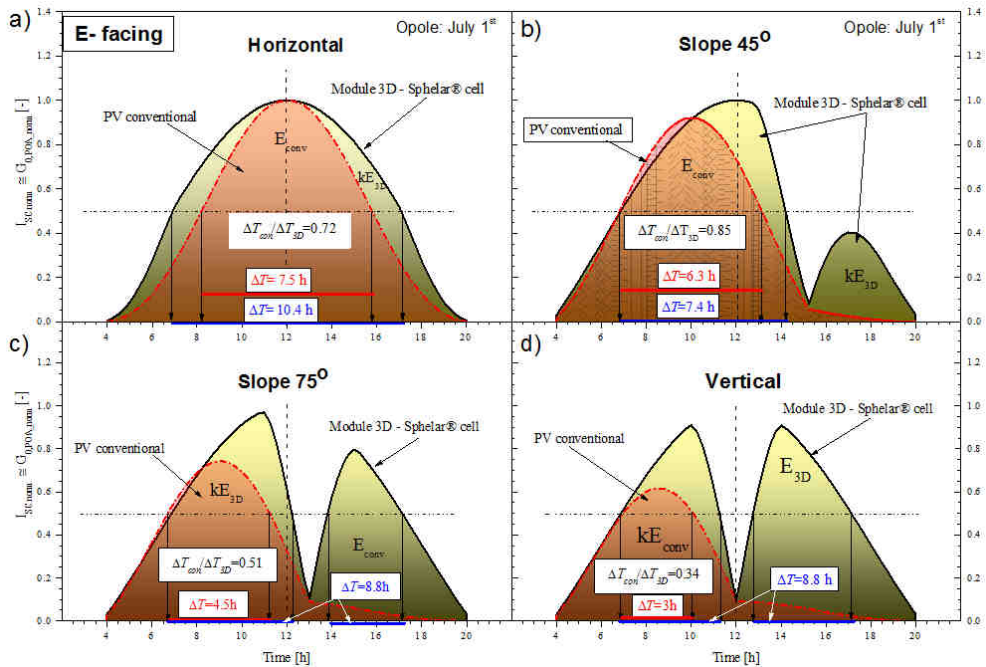


Fig. 13. Determine the effective work time of the modules from the normalized I_{sc} curves depending on the inclination angle of the modules. Normalisation were made to maximum of I_{sc} in horizontal position, for: the modules of the SPHELAR[®] cells with two active surfaces and a typical photovoltaic module with one active surface. Modules are oriented to the east and: a) horizontal; b) 45°; c) 75° and d) vertical

5. Table 1 shows the percent change in charge generation capability of the studied modules as a function of their inclination and orientation. As reference, the value of the generated charge in the horizontal position was assumed for each of them. In contrast, Table 2 shows the percentage gain of the charge (energy) that is obtained when replacing the flat conventional module with SPHELAR[®] module with the same I_{sc} current (nominal power) - as a function of γ angle starting from the horizontal position.

The analysis of the data shows that the SPHELAR[®] cell modules have a higher stability of charge generation capability independent of angle of inclination and orientation towards conventional modules. In the case of conventional modules, they are suitable only for operation in the southern orientation with optimum slope (e.g. for Southern Poland areas of 28-35°). Working in a different setting significantly worsens the generation of charge/energy. For example, work in the vertical southern position causes the charge/energy generation capability to drop to 45.3% of the horizontal setting, in comparison to 69.6% for the SPHELAR[®] cells. On the other hand, vertical/west position operation results in a decrease in generation capacity to 45.7% of the horizontal setting, where for the SPHELAR[®] cells is 87.9%. In such situation, the gain from replacement of the conventional module to the SPHELAR[®] module is 24.3% for south and 42.2% for east/west (see Table 2).

Table 1

Charge generation capability by inclined modules for angle γ with respect to horizontal position and south and east/west direction

Position	Type of modules	Charge generation capability	Inclination (γ)				
			0°	28°	45°	75°	90°
South	3D modules	[%]	100	95.9	93.7	86.7	69.6
	conventional PV	[%]	100	104	96.3	65.7	45.3
East/West	3D modules	[%]	100	91.3	88.2	87.9	87.9
	conventional PV	[%]	100	91.2	80.3	57.8	45.7

Table 2

The profit of the SPHELAR[®] module use compared to the standard PV in the function of γ angle. Modules were directed to the south (0°) and east (-90°)/west (+90°)

Position	Profit from the use of 3D modules	Inclination (γ)				
		0°	28°	45°	75°	90°
South	[%]	0	-8.1	-2.6	21	24.3
East/West	[%]	0	0.1	7.9	29.2	42.2

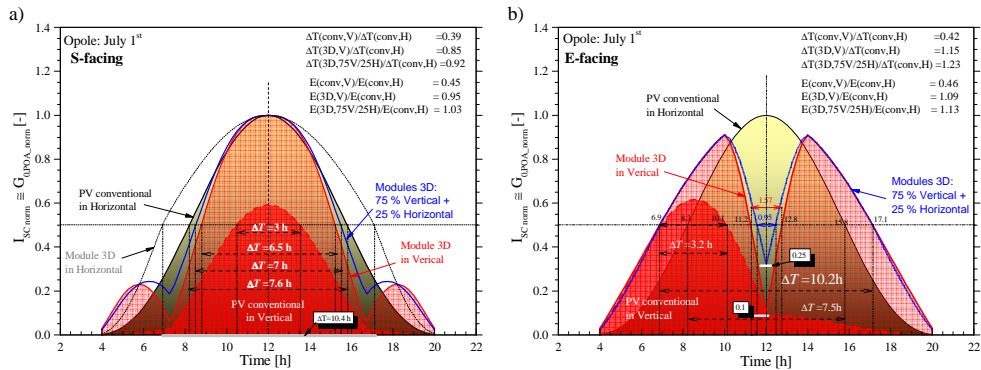


Fig. 14. The effective working time of the selected modules and the gain of the accumulated charge (energy) with respect to the horizontally arranged conventional module of the same power and nominal current, for: a) southern facing, b) eastern facing. Normalisation were made to maximal I_{SC} current value of the module obtained in the horizontal position

Figure 14 and Table 3 show the comparison of effective modules' work times and accumulated energy gains relative to the horizontally positioned conventional module with the same power and nominal current for: a) southern setting; b) eastern setting. The simulation was performed for: a conventional vertical module, a SPHELAR[®] cell module in a vertical setting, a set of two connected modules with SPHELAR[®] cells: the first one - vertically aligned with 75% of the total power of the set with the second horizontally arranged having 25% power of the set. In research, normalization was made to maximum I_{SC} current value of the tested module from the horizontal position. The analysis of the results presented in Figure 14 and Table 3 gives the following observations:

1. Modules orientated vertically in the east/west direction always have lower current values, I_{SC} , relative to their horizontal orientation, wherein the ability to generate charge/energy of 3D modules is twice as much as conventional modules. In the case of

3D modules, they achieve up to 109% of the charge/energy values obtained by the conventional module in a horizontal setting, where conventional modules only achieve 46%.

Table 3

A summary of the effective working times of modules and cumulative charge (energy) gains with respect to a horizontally arranged conventional module with the same power and nominal current

Type	Azimuth	Effective working time with respect to PV conv. in horizontal	Generation capability with respect to PV conv. in horizontal
PV conventional in vertical	South	0.39	0.45
	East / West	0.42	0.46
3D modules in vertical	South	0.85	0.95
	East / West	1.15	1.09
Set of: 75% P_m of 3D modules in vertical + 25% P_m of conventional PV modules in horizontal	South	0.92	1.03
	East / West	1.23	1.13

- By determining the effective working time of the module as a time when the value of the generated photocurrent exceeds half of the value obtained at midday, it is determined that the 3D modules aligned vertically in the east/west direction works 15% longer than the typical conventional modules set horizontally. Such features do not have conventional PV modules (Fig. 7b) - 58% reduction in effective working time is achieved.
- Extension of the effective work time of modules is very important in particular when planning when they are used in autonomous photovoltaic systems. Then when using typical PV modules due to the need to obtain the assumed power value from the module in early morning hours (late evening) it is necessary to use a very high redundancy of installed modules power. This causes that in the midday hours the potential energy available from these modules is not used. In this context, in some applications, the ability to prolong the effective work time of a module at the expense of decreasing energy output from around midday is a very valuable feature.
- SPHELAR[®] modules are ideally suited for the construction of a set of connected modules: one vertically aligned with the other horizontally positioned, which allows for easy modelling of their I-U characteristics due to changes in power distribution proportions in the components (see Fig. 14). The charge/energy accumulation capability of this set of connected modules, having the same power and nominal current as the reference module (see Table 3), always exceeds the charge/energy values obtained for the horizontal orientation of the conventional PV module while maintaining a significant elongation of the effective work time.

The above simulations fully coincide with open field research. The results of short-term and long-term open-area studies for modules located in the vertical orientation of south and east, together with a comparison of their properties with respect to the conventional module, are presented in [9, 10].

Summary and conclusions

These research results are presented in simplified assumptions. They assume the same ability to work in small irradiation conditions of both modules, although the results obtained in [1, 2] have shown that SPHELAR[®] cell modules have much better performance.

With such assumptions, the occurrence of the phenomenon of elongation of the effective SPHELAR[®] module operating time, set vertically in the east/west direction, is over 50% in comparison to the horizontal orientation of the typical PV module (for summer months). Additionally the ability to modelling the current characteristics of the sets of connected modules open up new possibilities for their application.

Due to the features discussed above, SPHELAR[®] cell modules can be used in new applications in building integrated photovoltaics, as elements of elevation in the form of photovoltaic facades, windows and roofs. In particular, as part of autonomous photovoltaic systems installed for reasons of safety at airports and noise barriers on motorways and expressways [11].

References

- [1] Rodziewicz T, Nakata J, Taira K, Zaremba A, Waclawek M. Performance of SPHELAR[®] Module at Outdoor Conditions in Higher Latitude Areas. Proc 23rd Europ Photovolt Solar Energy Conf. 2008;596-599. DOI: 10.4229/23rdEUPVSEC2008-1CV.2.60.
- [2] Rodziewicz T, Nakata J, Taira K, Zaremba A, Waclawek M. Performance of Flat Module Made of SPHELAR[®] Cells in Higher Latitude Areas. Proc 24th Europ Photovolt Solar Energy Conf. 2009;3513-3516. DOI: 10.4229/24thEUPVSEC2009-4AV.3.63.
- [3] Waclawek M, Rodziewicz T. Ogniwa słoneczne. Wpływ środowiska naturalnego na ich pracę (Solar cells. The impact of the natural environment on their work). 2nd edition. Warszawa: WNT; 2014. ISBN: 978-83-7926-264-9.
- [4] Spencer JW. Fourier Series Representation of the Position of the Sun. Search. 1971;2:162-172.
- [5] Kaiser H. Wykorzystanie energii słonecznej. Kraków: Wydawnictwo AGH; 1995.
- [6] Myers DJ. Solar Applications in Industry and Commerce. Englewood Cliffs, New Jersey: Prentice-Hall, Inc. 1984.
- [7] Whitaker C, Newmiller J. Photovoltaic Module Energy Rating Procedure. Final Subcontract Report. San Ramon, California: Newmiller Endecon Engineering; NREL contract No. DE-AC36-83CH10093, January 1998.
- [8] Commission for Instruments and Methods of Observation. Abridged Final Report of the Eighth Session. Geneva: World Meteorological Organization. https://library.wmo.int/pmb_ged/wmo_590_en.pdf.
- [9] Imoto S, Taira K, Nakata J, Inagawa I, Ohtani S. Transparent and bifacial SpheLAR[®] panel. Proc 25th Europ Photovolt Solar Energy Conf. 2010;241-244. DOI: 10.4229/25thEUPVSEC2010-1CO.7.3.
- [10] Taira K, Nakata J, Inagawa I, Ohtani S. A new benchmark required for SpheLAR[®] technology. Proc 25th Europ Photovolt Solar Energy Conf. 2010;562-566. DOI: 10.4229/25thEUPVSEC2010-1DV.3.1
- [11] Popławski T, Szelaąg P, Głowiński C, Adamowicz Ł. Forecast of Electric Power Generated by the Wind Farm Using Data Clustering Method. In: Information Systems Architecture and Technology. Knowledge Based Approach to the Design, Control and Decision Support. Wrocław: Ofic Wyd Politechniki Wrocławskiej; 2013;175-184. ISBN: 978-83-7493-802-0.